

MINIMUM RETURN DIFFERENCE AS A COMPENSATOR DESIGN TOOL

THOMAS J. CAVICCHI

Dept. of Electrical and Computer Engineering

Grove City College

Grove City, PA 16127-2104

Supplementary materials

Note: I discovered a minor typo in the paper. On p. 126, run 3, the achieved steady-state error is 0.1, not 0.05. Note also that I should have explicitly mentioned in the paper, though it is obvious in Fig. 6a, upper figure, that without compensation the closed-loop system is unstable for the value of gain set for 0.1.
11/13/2001

1: EXPANDED FIG. 3 (on the following page).

For brevity, the figures below were included for only one plant in the paper. Showing here results for a greater variety of plants demonstrates the validity of the RD_{\min} approximation and enhances understanding of the relation between GM and PM (in particular, that that relation is plant-dependent).

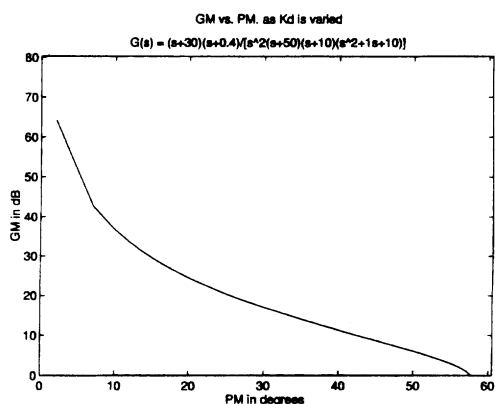
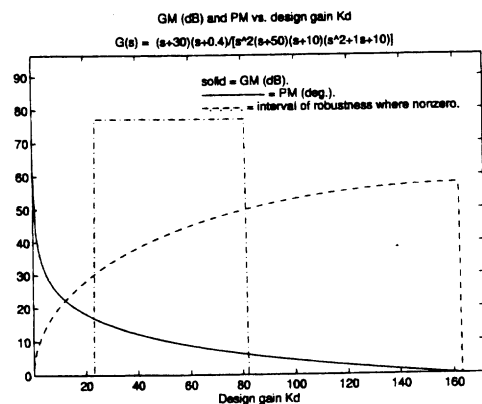
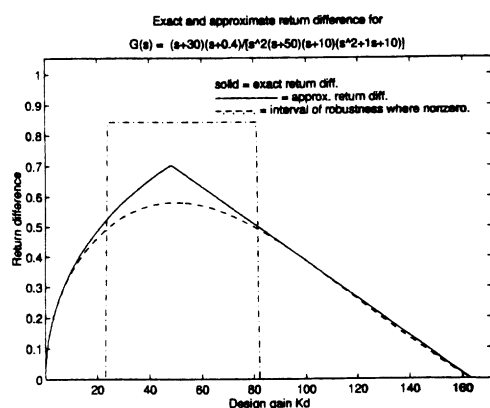
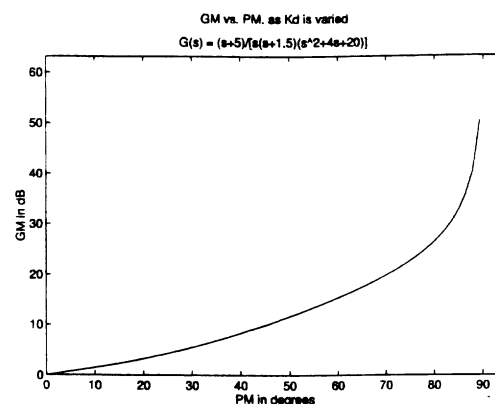
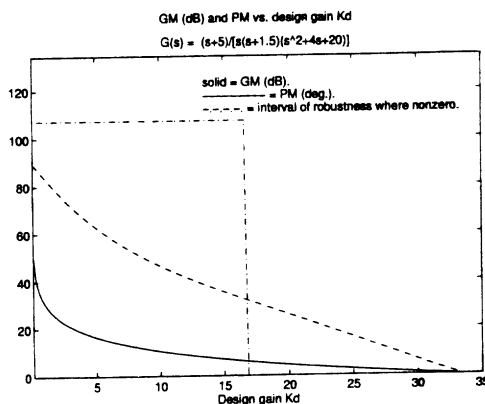
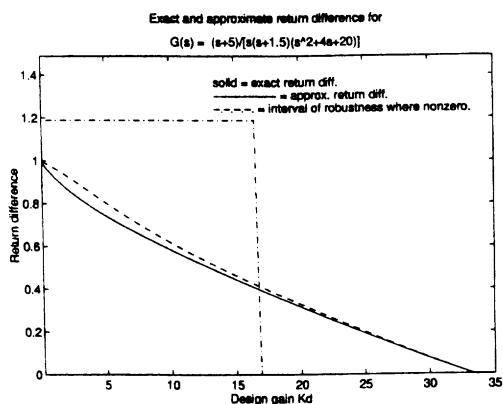
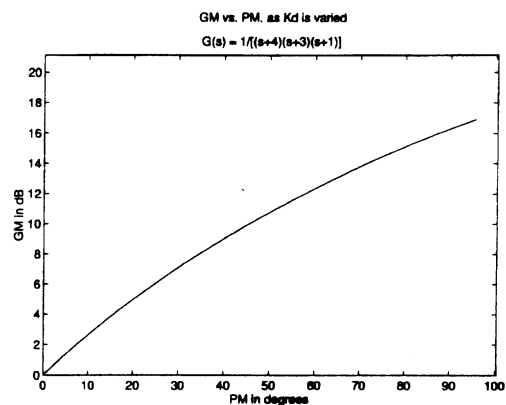
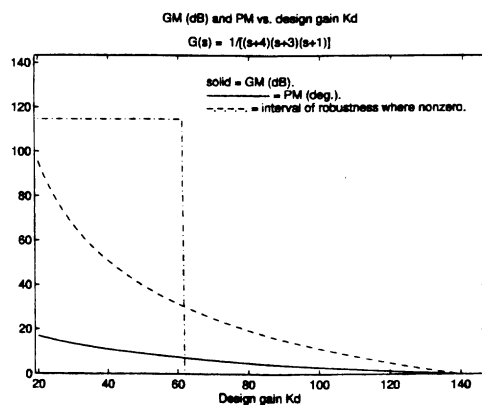
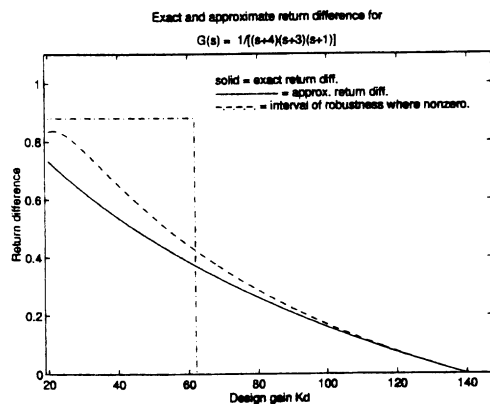
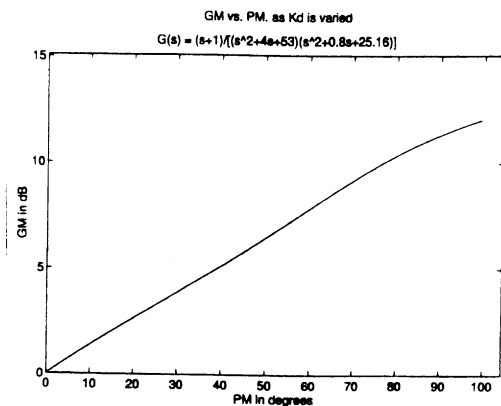
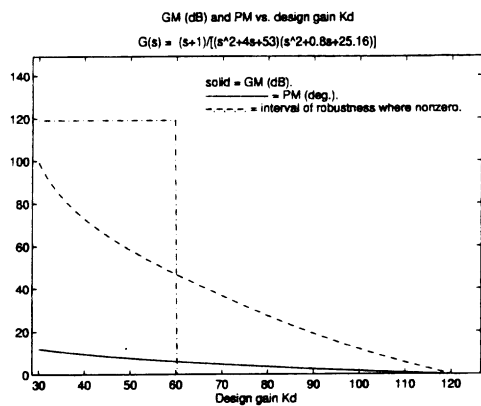
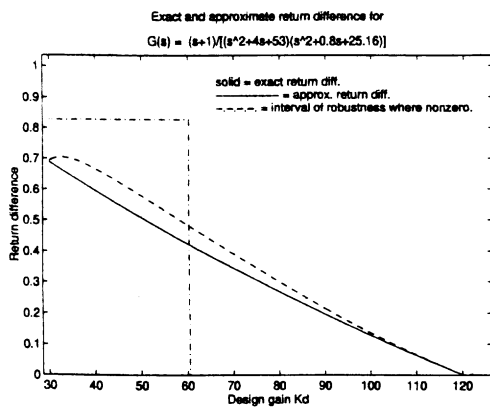
Each plot in a row pertains to the same plant (in the plots, K_m is referenced by K_d):

(a, left column) Approximate RD_{\min} and exact RD_{\min} vs. gain K_m .

(b, center column) $GM(K_m)$ and $PM(K_m)$ vs. K_m .

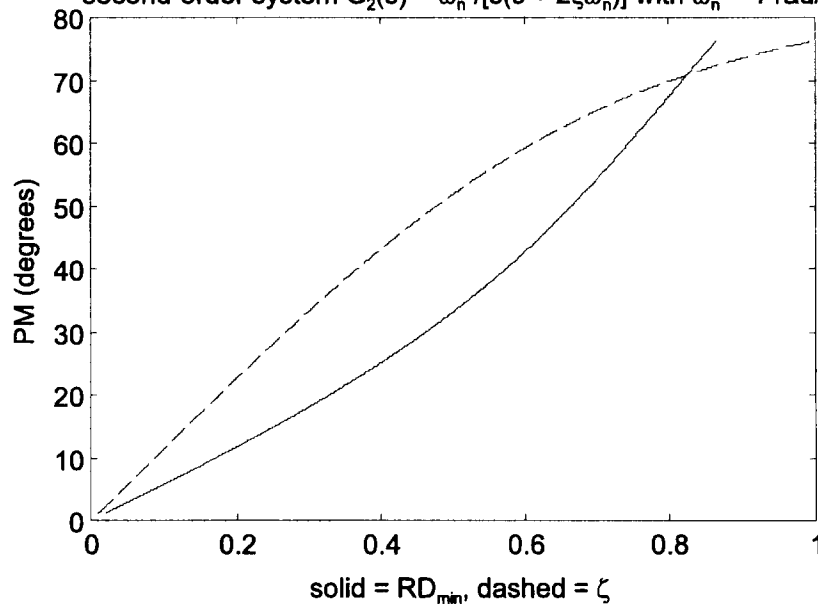
(c, right column) $GM(K_m)$ vs. $PM(K_m)$.

Note that numerous stylistic improvements have been made on the graphs in Fig. 3 of the paper relative to those shown here.



2: PLOT OF PM VS. RD_{min} AND OF PM vs. ζ FOR $G_2(s) = \omega_n^2/[s(s+2\zeta\omega_n)]$ with $\omega_n = 1$ rad/s and $K_m = 1$. Notice that PM rises with both RD_{min} and ζ , for $G(s) = G_2(s)$. Remember, however, that these plots are valid ONLY for the second-order canonical system with $K_m = 1$! Also, although ω_n was set to 1 rad/s to numerically specify $G_2(s)$ in the figure below, the value of ω_n does not affect the plots (ω_n affects only ω_0 , ω_{gc} , and other critical frequencies via linear scaling of them).

Phase margin (PM) vs. RD_{min} and PM vs. damping ratio ζ for canonical second-order system $G_2(s) = \omega_n^2/[s(s + 2\zeta\omega_n)]$ with $\omega_n = 1$ rad/s.



3: EXPANDED FIG. 6 (on the following pages).

All these graphical simulation results are for the trials quantitatively described in Table I of the paper; Fig. 6 shows only two of these 20 runs, each of which may include both a lead and a lag design. For brevity, graphical results for all the other runs were omitted from the paper but are presented below. Showing here a greater variety of plants demonstrates the versatility of the RD-based compensator design algorithm and serves to compare it with the conventional PM-based Bode design procedures for lag and lead compensators.

Each plot in a row pertains to the same plant (in the plots, K_m is referenced by K_d):

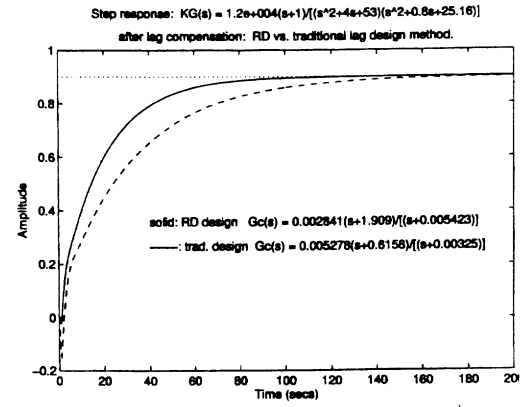
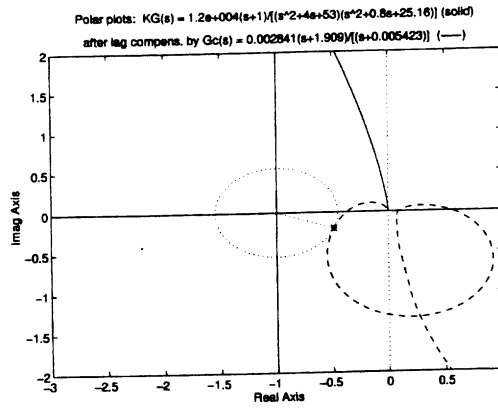
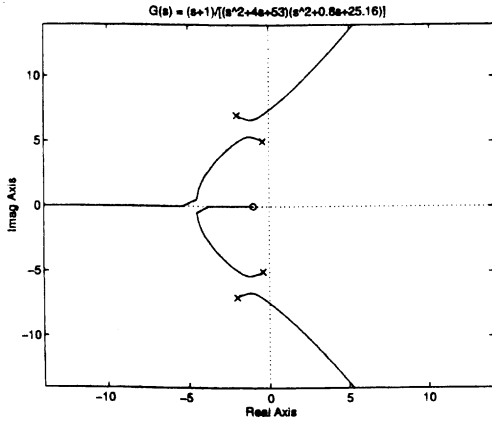
(a, left column) Root locus.

(b, center column) Polar plots of uncompensated and RD-compensated systems.

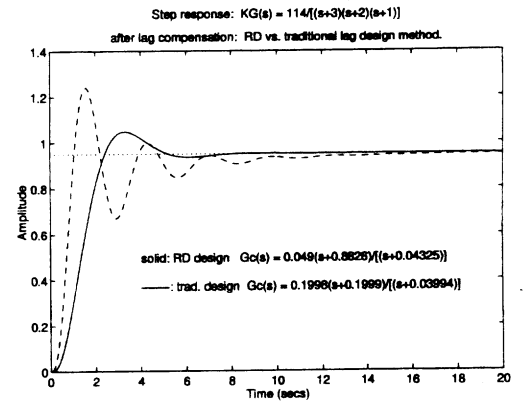
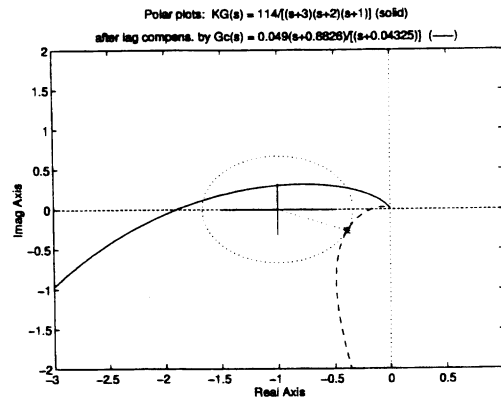
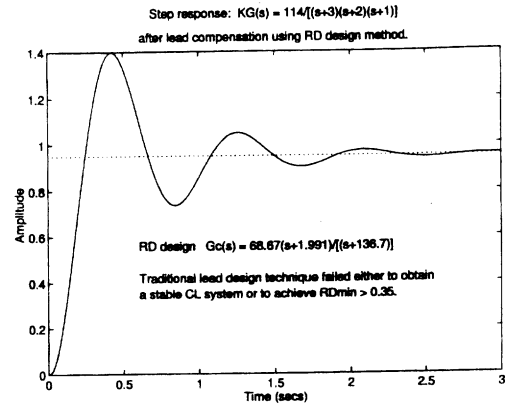
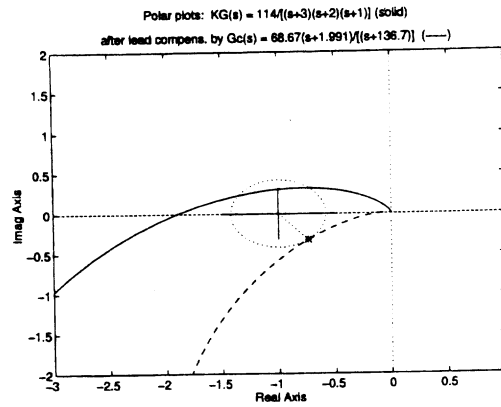
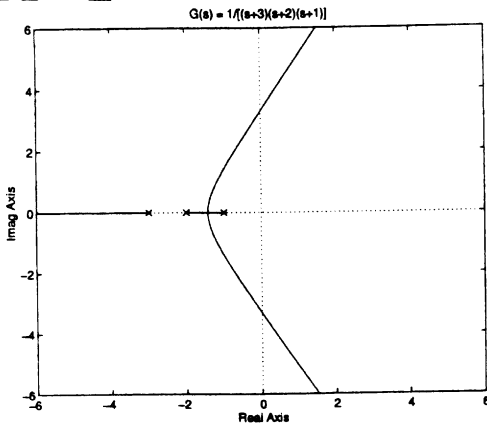
(c, right column) Closed-loop step response simulation comparisons.

Note that numerous stylistic improvements have been made on the graphs in Fig. 6 of the paper relative to those shown here.

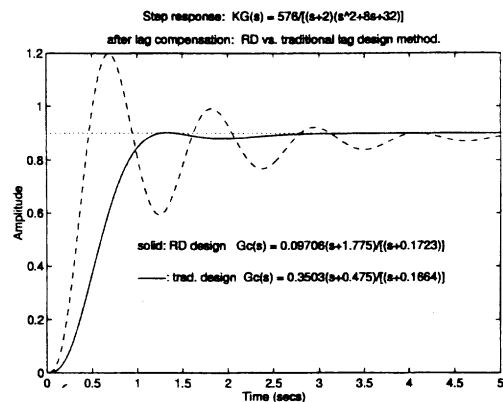
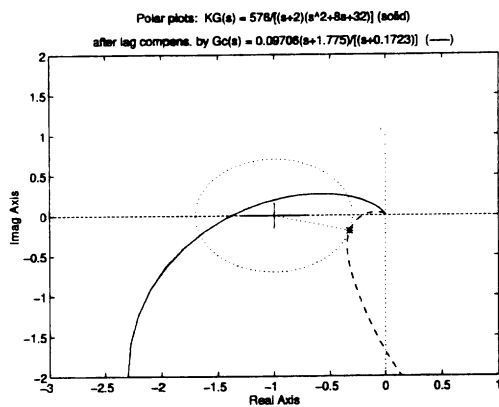
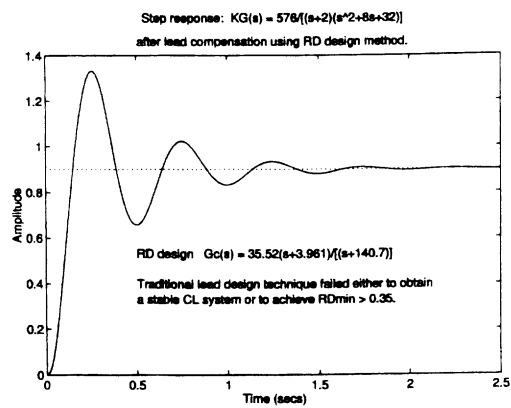
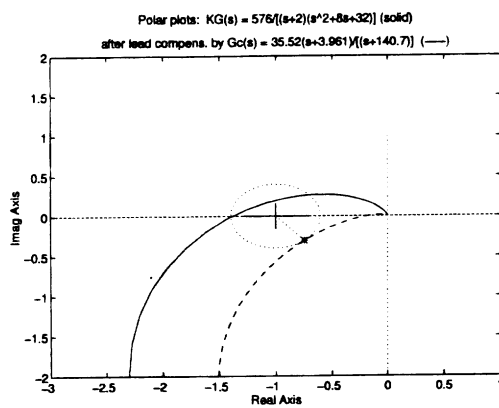
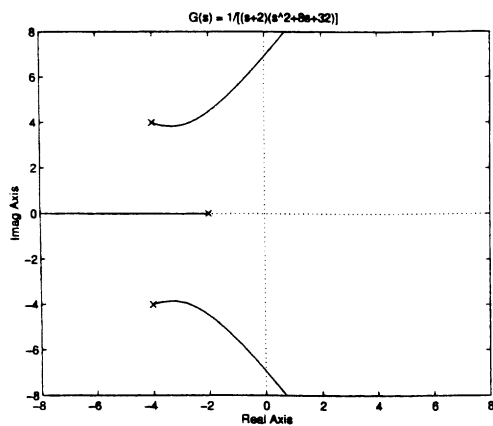
TF 1



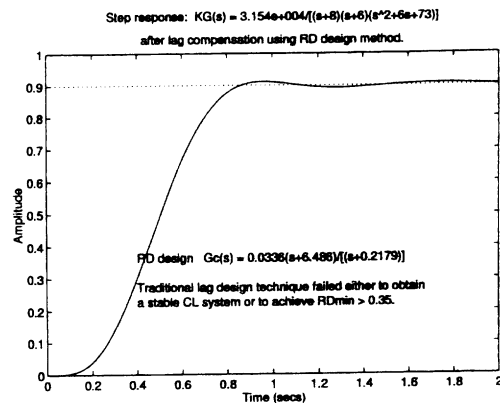
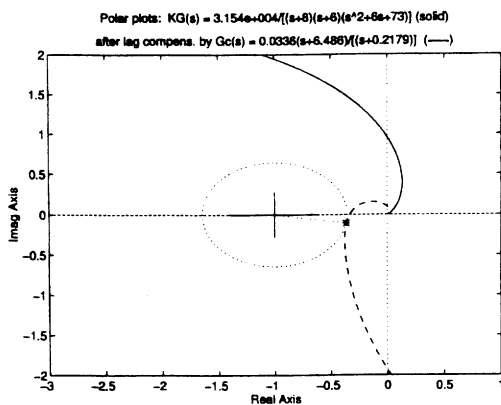
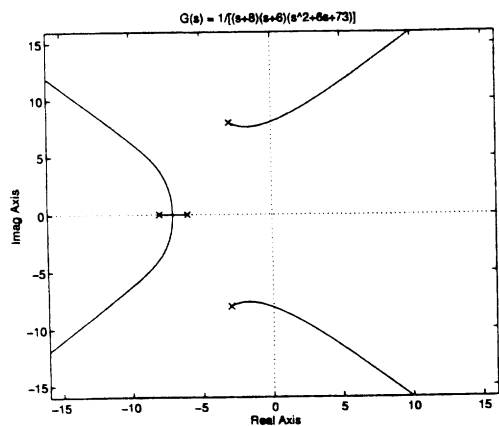
TF 2



TF 3

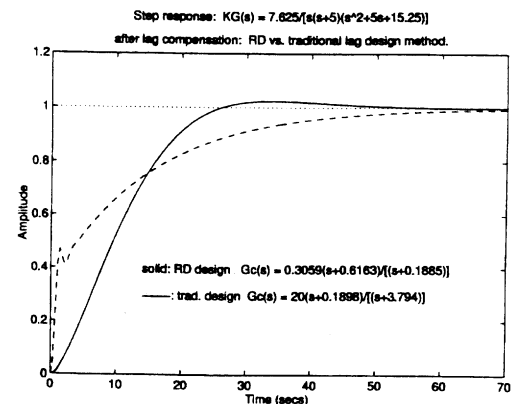
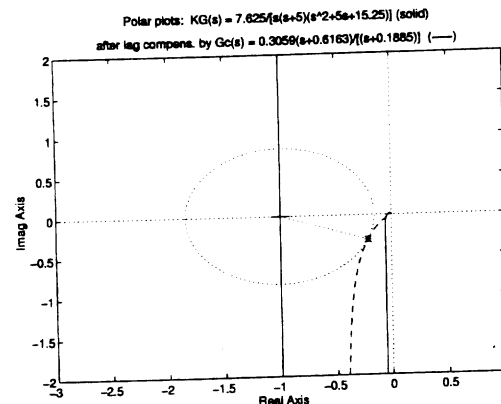
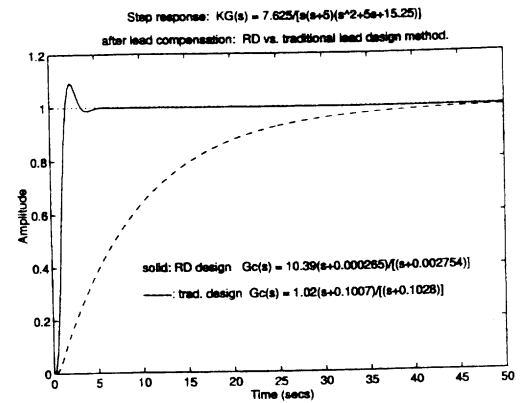
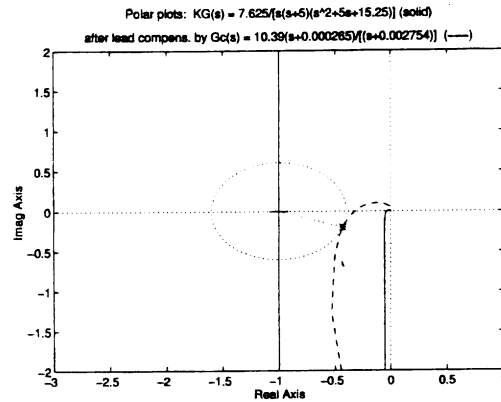
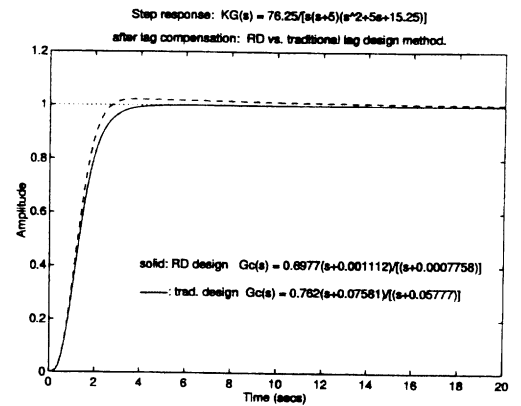
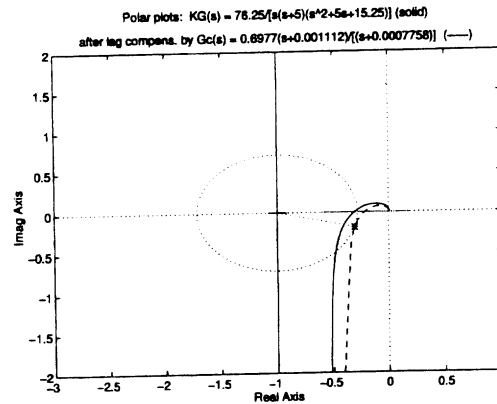
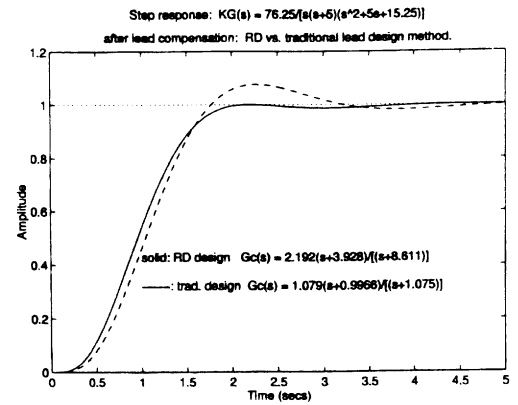
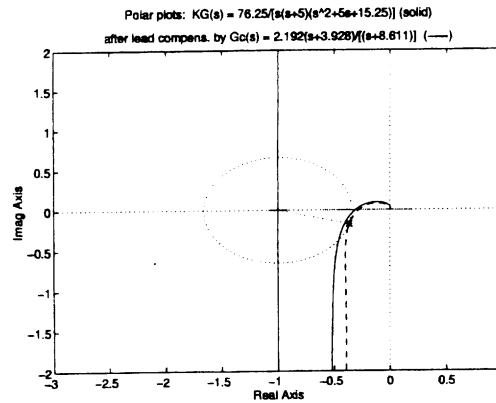
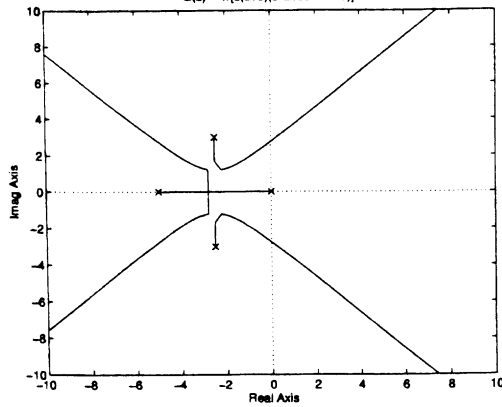


TF 4

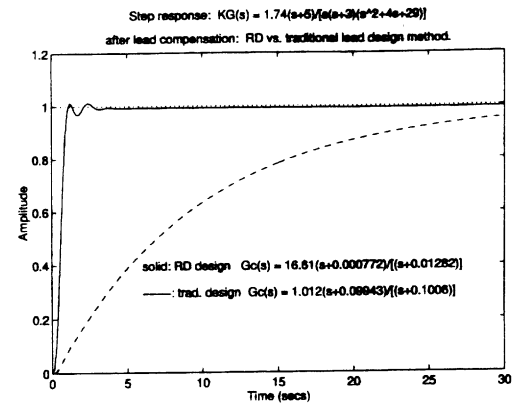
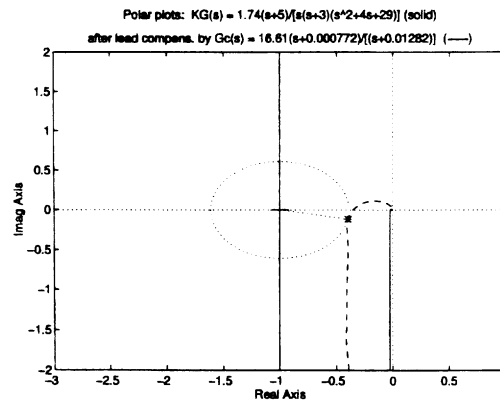
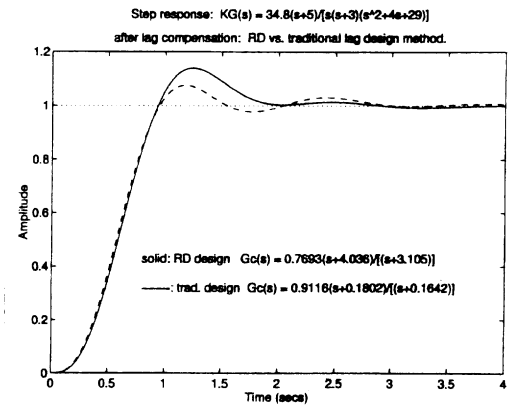
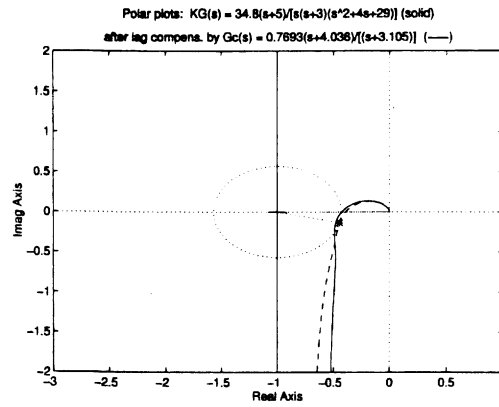
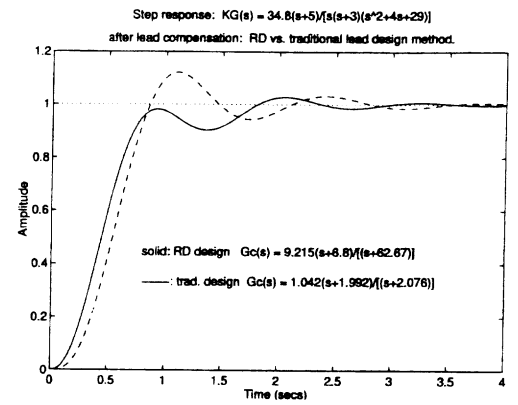
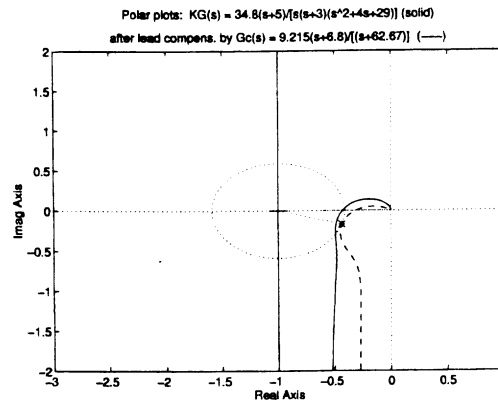
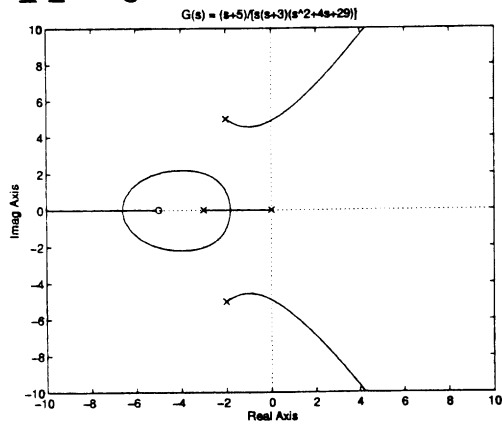


TF 5

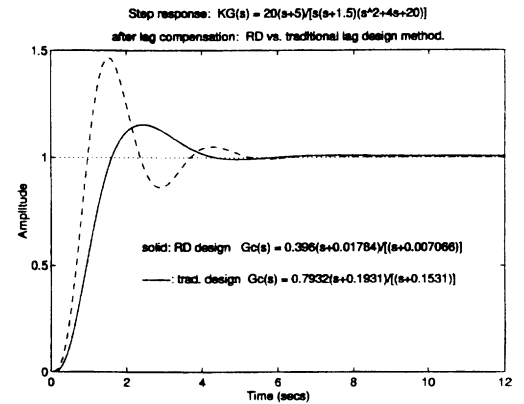
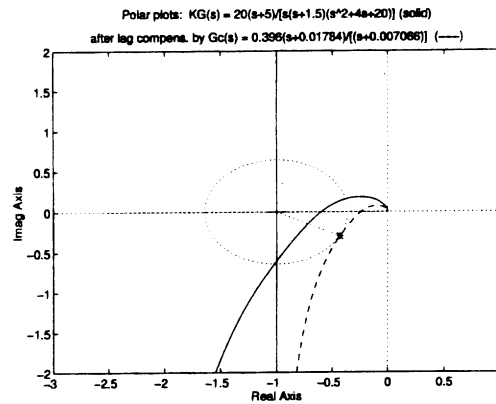
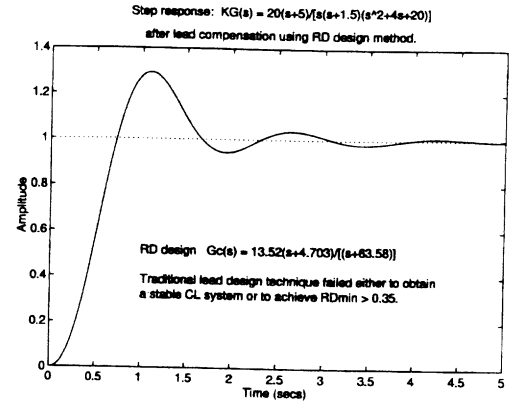
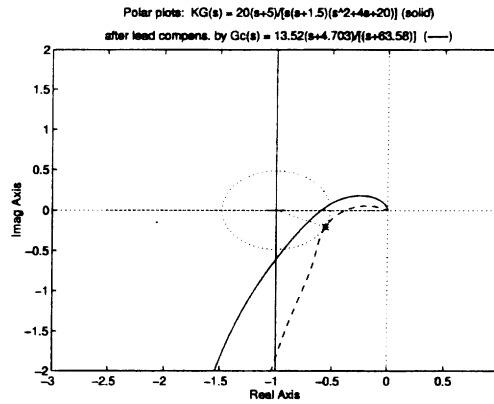
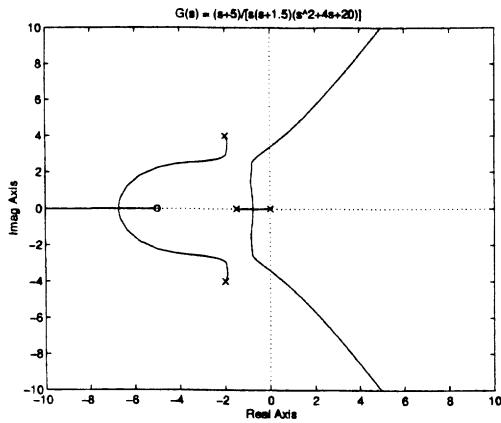
$$G(s) = 1/(s(s+5)(s^2+5s+15.25))$$



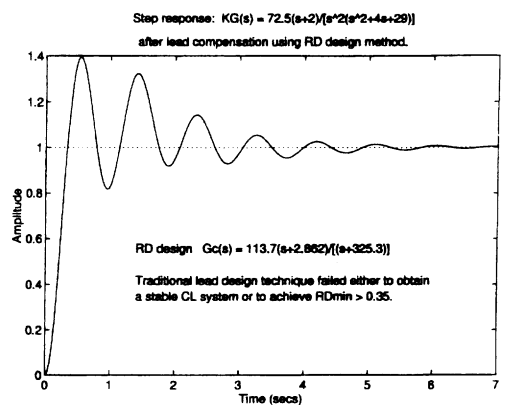
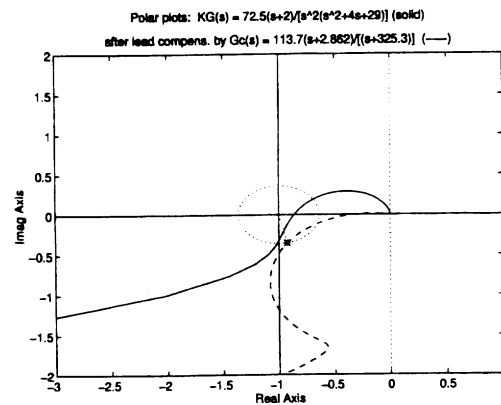
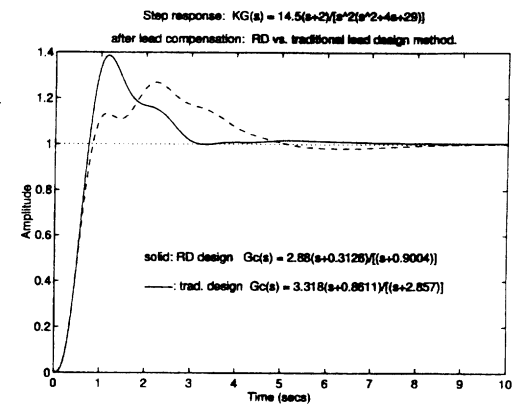
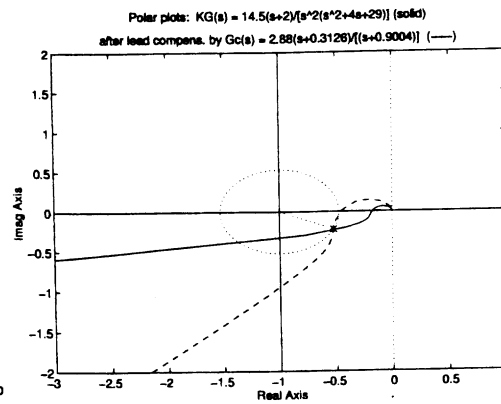
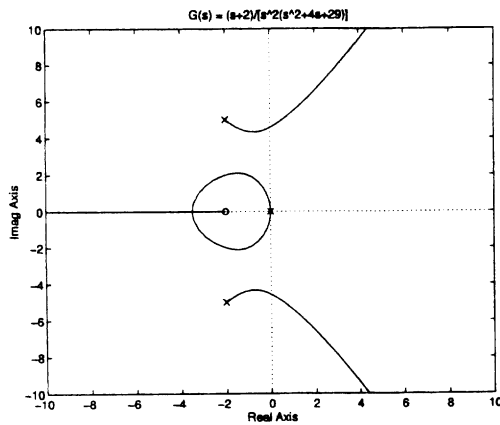
TF 6



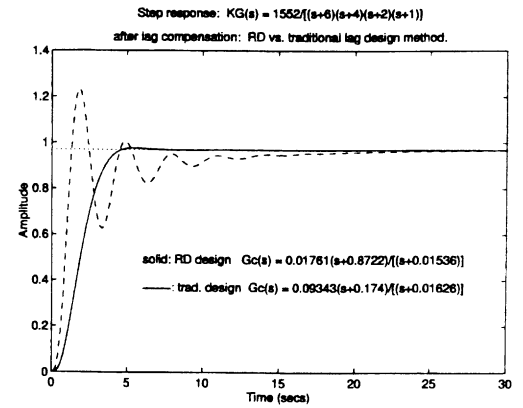
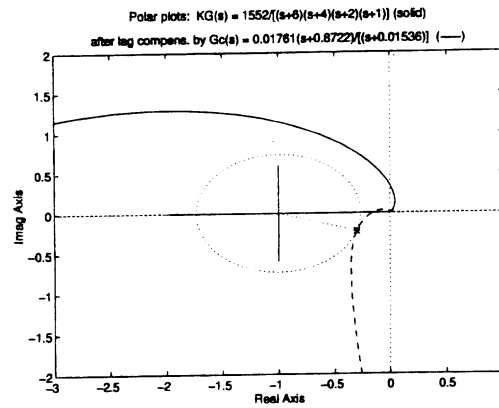
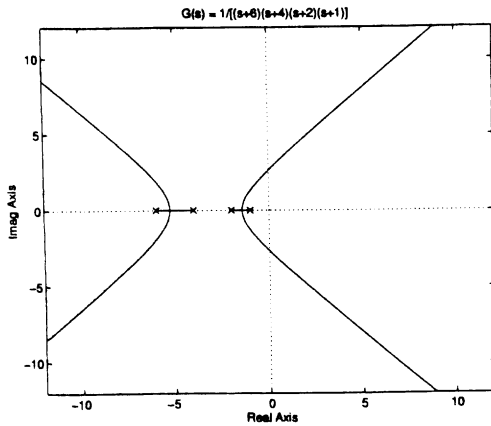
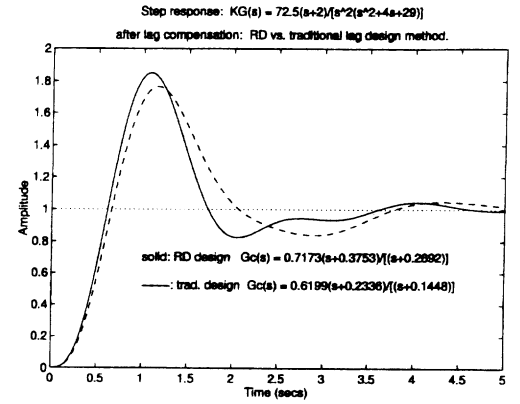
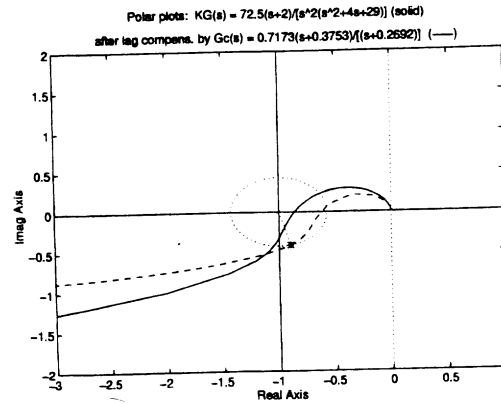
TF 7



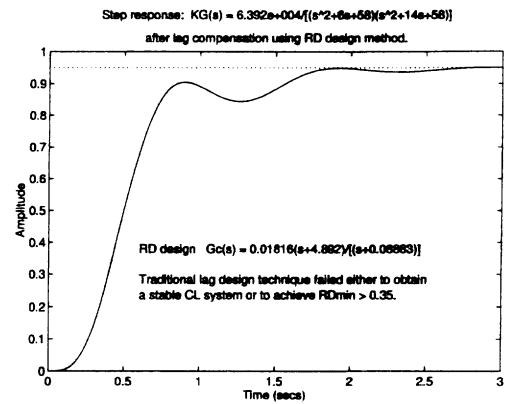
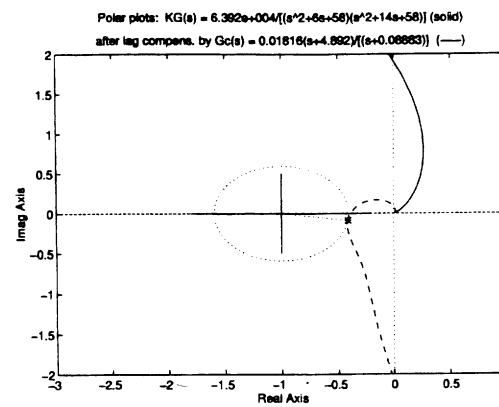
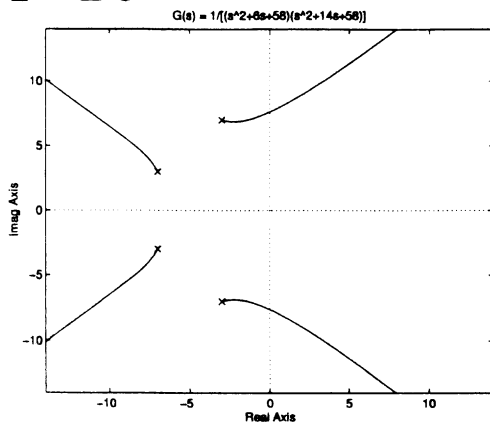
TF 8



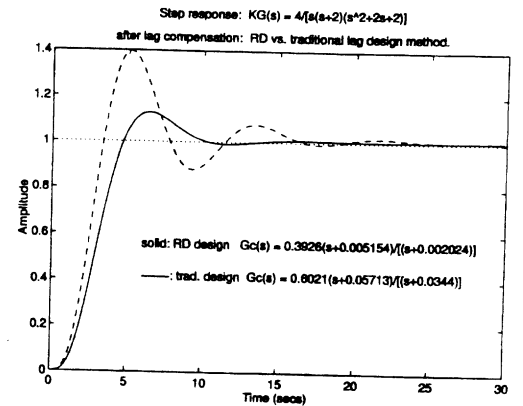
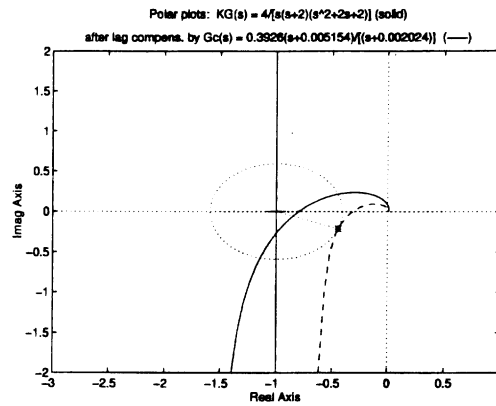
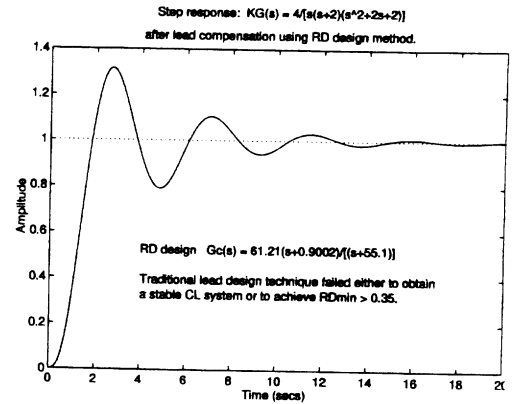
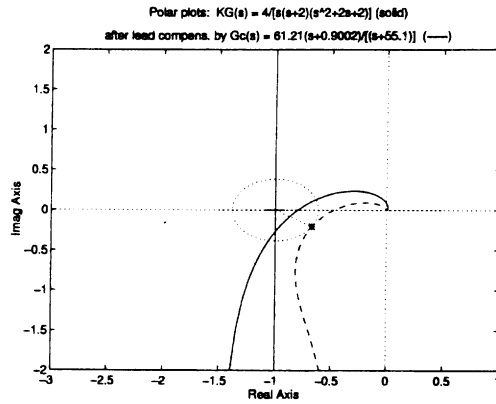
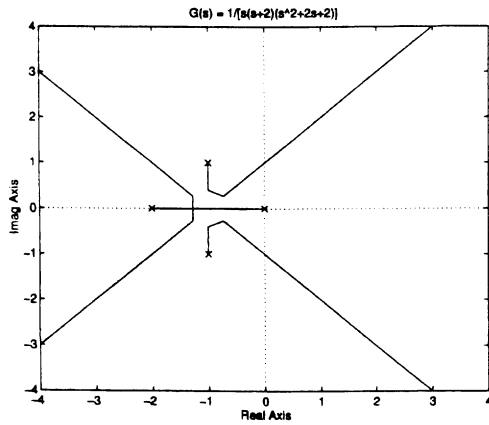
TF 9



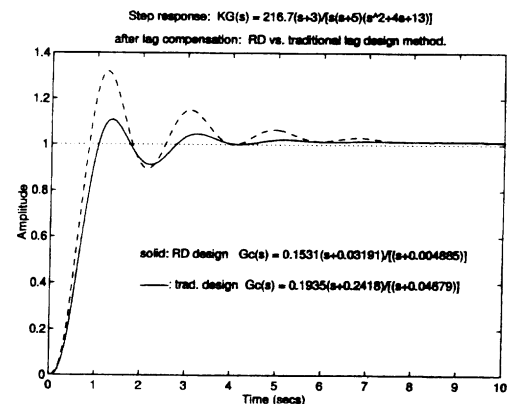
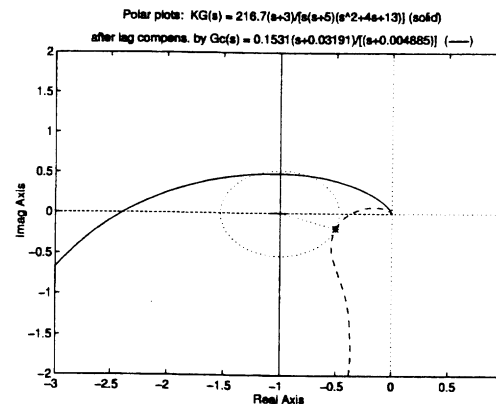
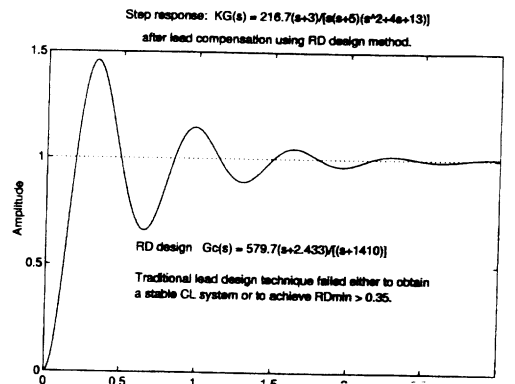
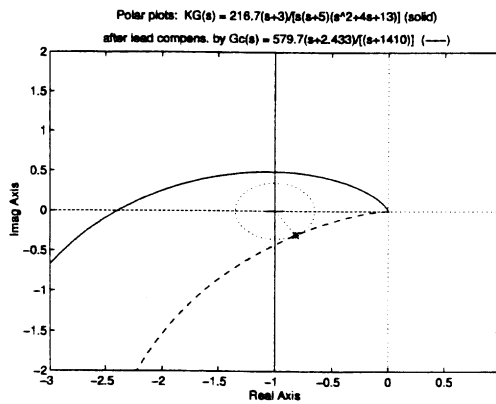
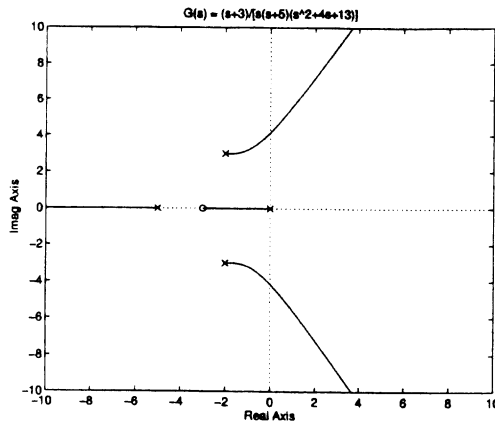
TF 10



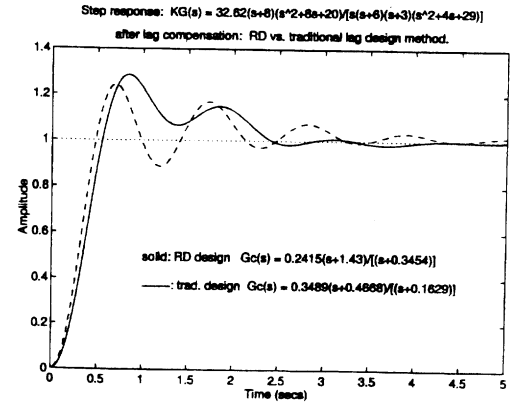
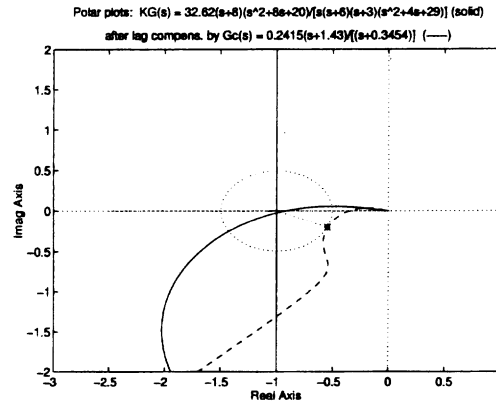
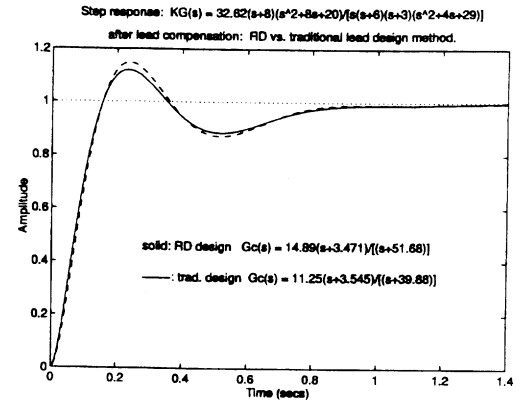
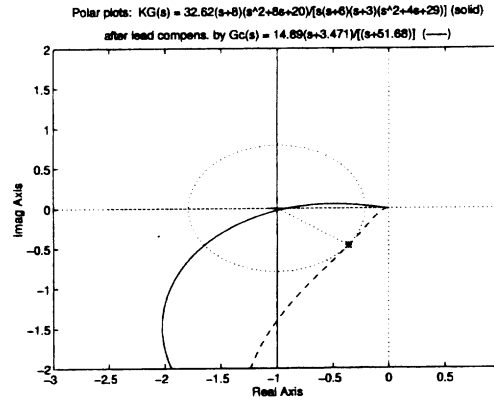
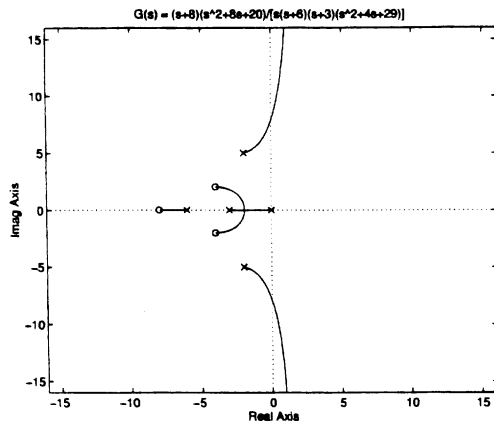
TF 11



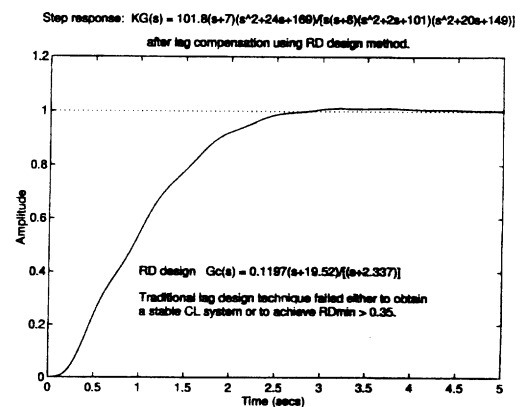
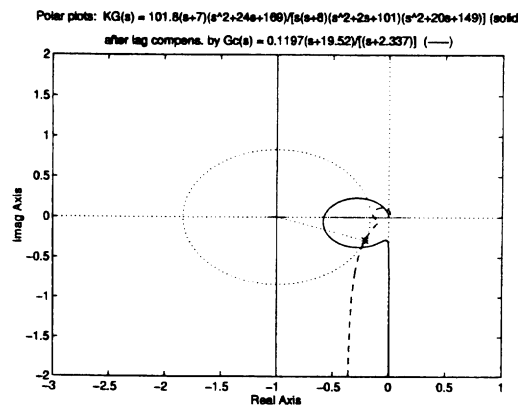
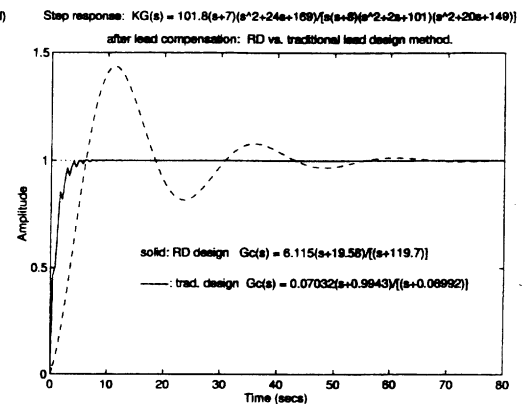
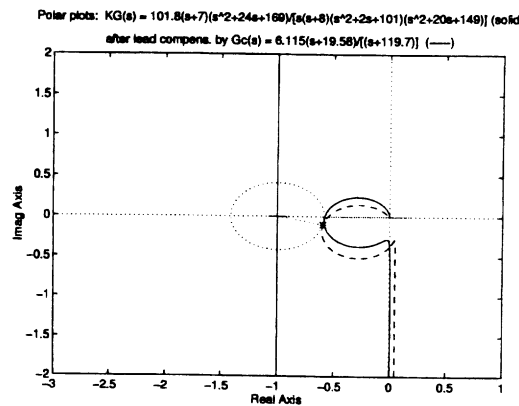
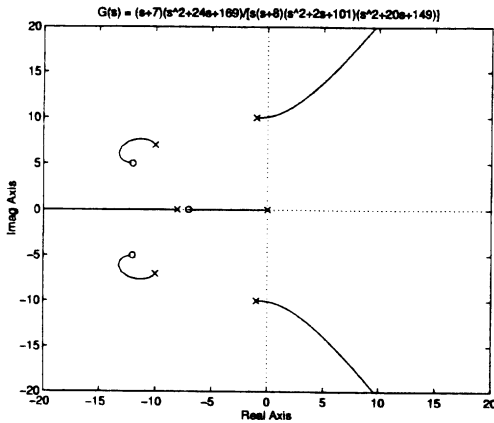
TF 12



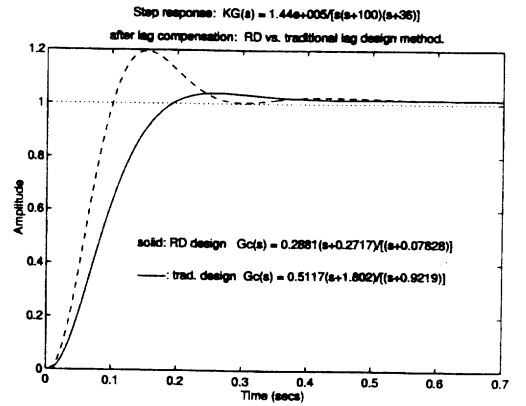
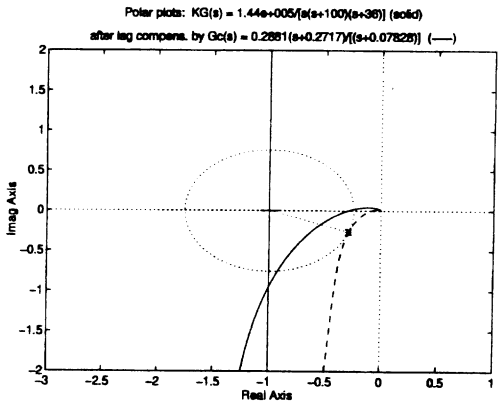
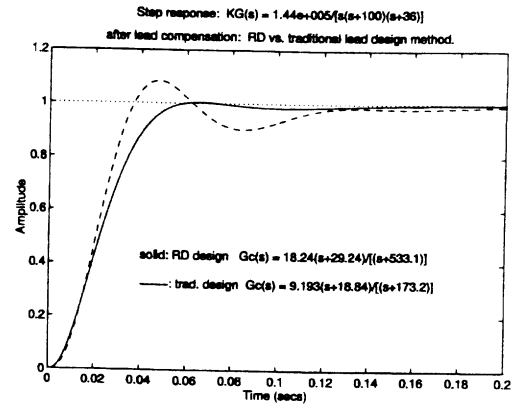
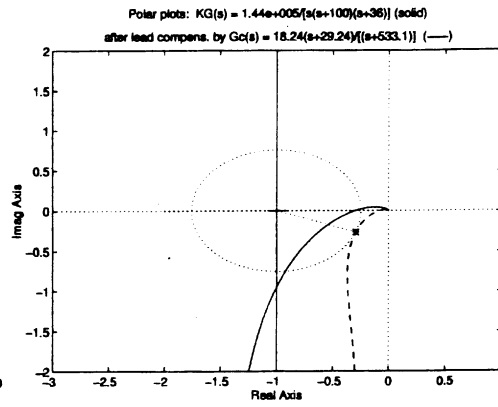
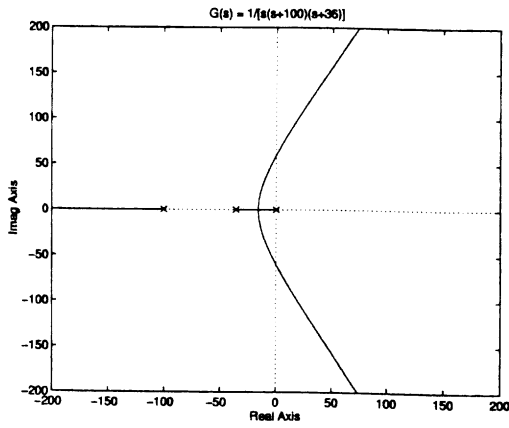
TF 13



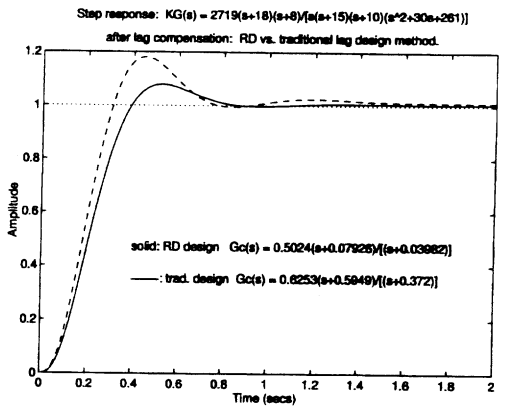
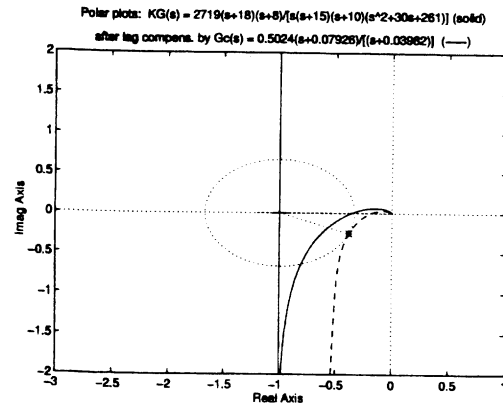
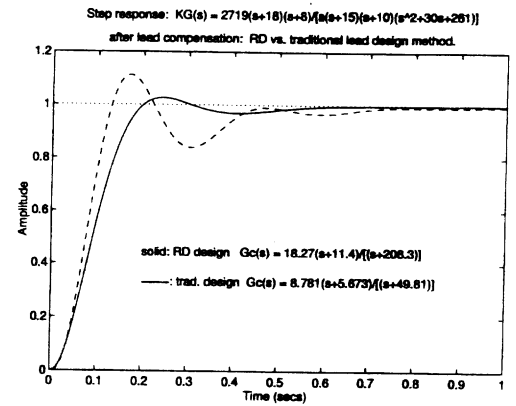
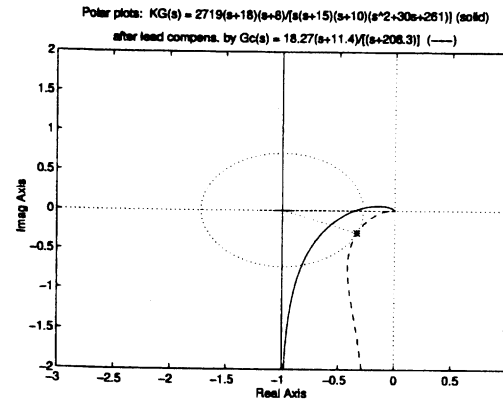
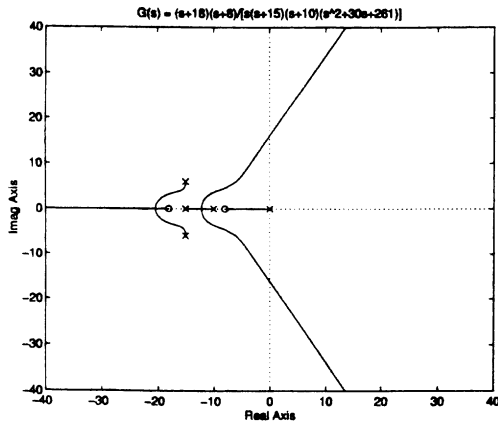
TF 14

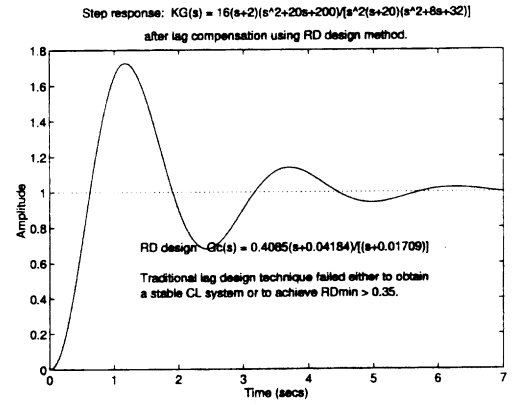
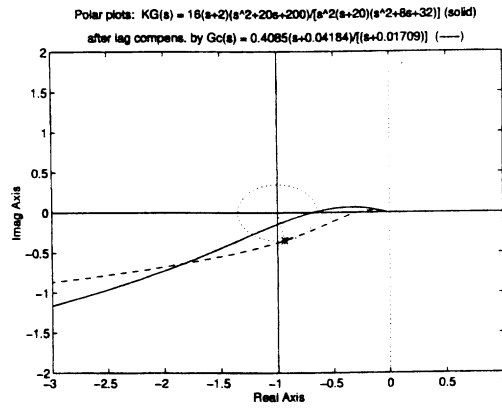
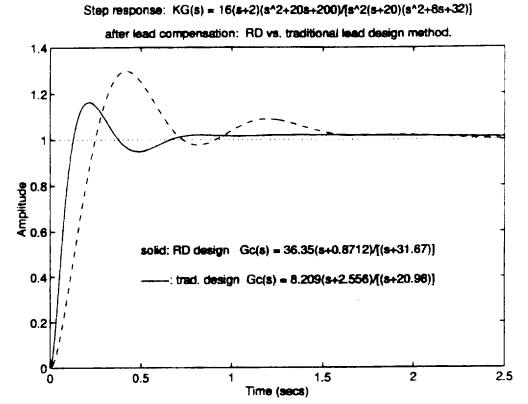
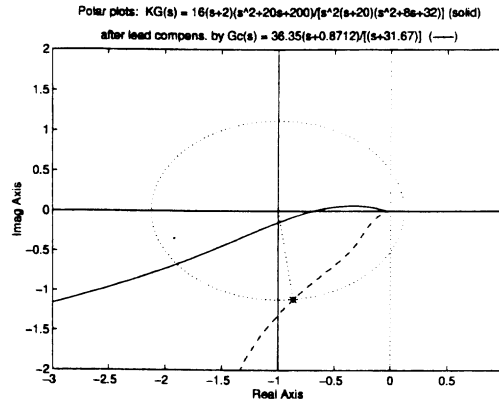
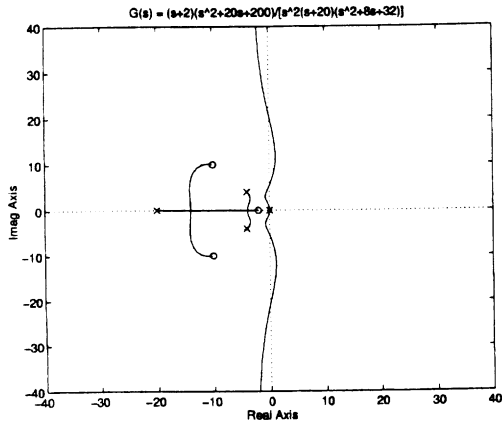


TF 15



TF 16





4: SEARCH RANGE REFINEMENTS FOR GREATER EFFICIENCY.

An example of increases in search efficiency possible in future versions of the algorithm (such as in a student project) is indicated in reference to Fig. a for lead designs and Fig. b (diagrams on the following pages) for lag designs. Notice that the systems, both uncompensated and compensated, are the same as in Fig. 4 of the paper: $G(s) = (s+5)/[s(s+1.5)(s^2+4s+20)]$ and $K_m = 20$; some of the details in Fig. 4 have been omitted, and new details have been added for this discussion. These plots show the uncompensated and compensated polar plots for $G(s)$, ω_0 , ω_1 , ω_0' , θ_1 , RD_1 , RD_{min} , and RD_{min}' . In Fig. a (lead), at a given candidate frequency ω_1 , the hatched areas show the possible movement of the polar plot point for ω_1 obtainable by adding a stable, minimum-phase lead compensator. This region is the intersection of the exterior of the $|K_m G(j\omega_1)|$ circle and counter-clockwise (CCW) from the ray at angle $\angle K_m G(j\omega_1)$, because the lead compensator increases both the magnitude and phase of $K_m G(j\omega_1)$. In general, it would be pointless to examine θ_1 (which is negative) more positive than θ_A , where θ_A is the (negative) angle from -1 to the (geometrically determinable) lower intersection of the RD_1 and $|K_m G(j\omega_1)|$ circles; in this case (due to small value selected for K_m for the particular steady-state error requirement), the circles do not intersect, so the most we could require is that θ_1 be less than θ_B . The general requirement $\theta_1 > \theta_A$ would have to be satisfied because all points on the selected RD_1 circle above θ_A are impossible to achieve with lead compensation, as they all fall within the $|K_m G(j\omega_1)|$ circle. The latter requirement $\theta_1 < \theta_B$ must hold because otherwise θ_1 would involve a phase lag, which a lead compensator cannot provide. Note that choosing $RD_1 > 0.4$ already will keep the compensated polar plot out of the nonrobust circle, as long as RD_{min} is not too much less than RD_1 . The reader might arrive at additional constraints on RD_1 , ω_1 , and θ_1 from this diagram. For example, if many such plots are done for different successful plants/compensated systems, patterns on the approximate relation between optimal θ_1 and ω_1 may emerge. For example, if ω_1 is selected, then the best θ_1 may typically be within a relatively narrow range for most plants and thus the search range for θ_1 may be further tightened. Note: As in the paper, RD_1 has artificially been made significantly larger than RD_{min}' and ω_1 has artificially been moved along the polar plot farther away from ω_0' ; the true location of ω_1 is indicated by an X with an arrow pointing into it. Notice that θ_1 in Fig. b now refers to the true location of ω_1 , unlike in the paper (as the reader now is sufficiently familiar with the diagram to make that transition). Also note from the discussion above about the limitations on what a lead compensator can do how if K_m is too large, the polar plot will extend beyond -1 and a first-order lead compensator will be unable to stabilize the system.

Similarly, in Fig. b, the region of possible movement by a lag compensator, the hatched region, is within the $|K_m G(j\omega_1)|$ circle and clockwise from the ray at angle $\angle K_m G(j\omega_1)$ because the lag compensator will reduce the gain and phase at $\omega = \omega_1$. It would similarly be pointless to examine designs with θ_1 more negative than θ_C , where θ_C is the (negative) angle from -1 to the intersection of the RD_1 and $|K_m G(j\omega_1)|$ circle closer to the positive real axis because all such θ_1 would be impossible to achieve with a lag compensator. Note: As in the paper, RD_1 has artificially been made significantly larger than RD_{min}' and ω_1 has artificially been moved along the polar plot farther away from ω_0' ; the true location of ω_1 is indicated by an X with an arrow pointing into it. Consequently, the artificial location of ω_1 in the compensated system actually violates the rule just established! But notice that the true location of ω_1 is within the hatched area. Notice, however, that θ_1 in Fig. b now refers to the true location of ω_1 , unlike in the paper (as the reader now is sufficiently familiar with the diagram to make that transition).

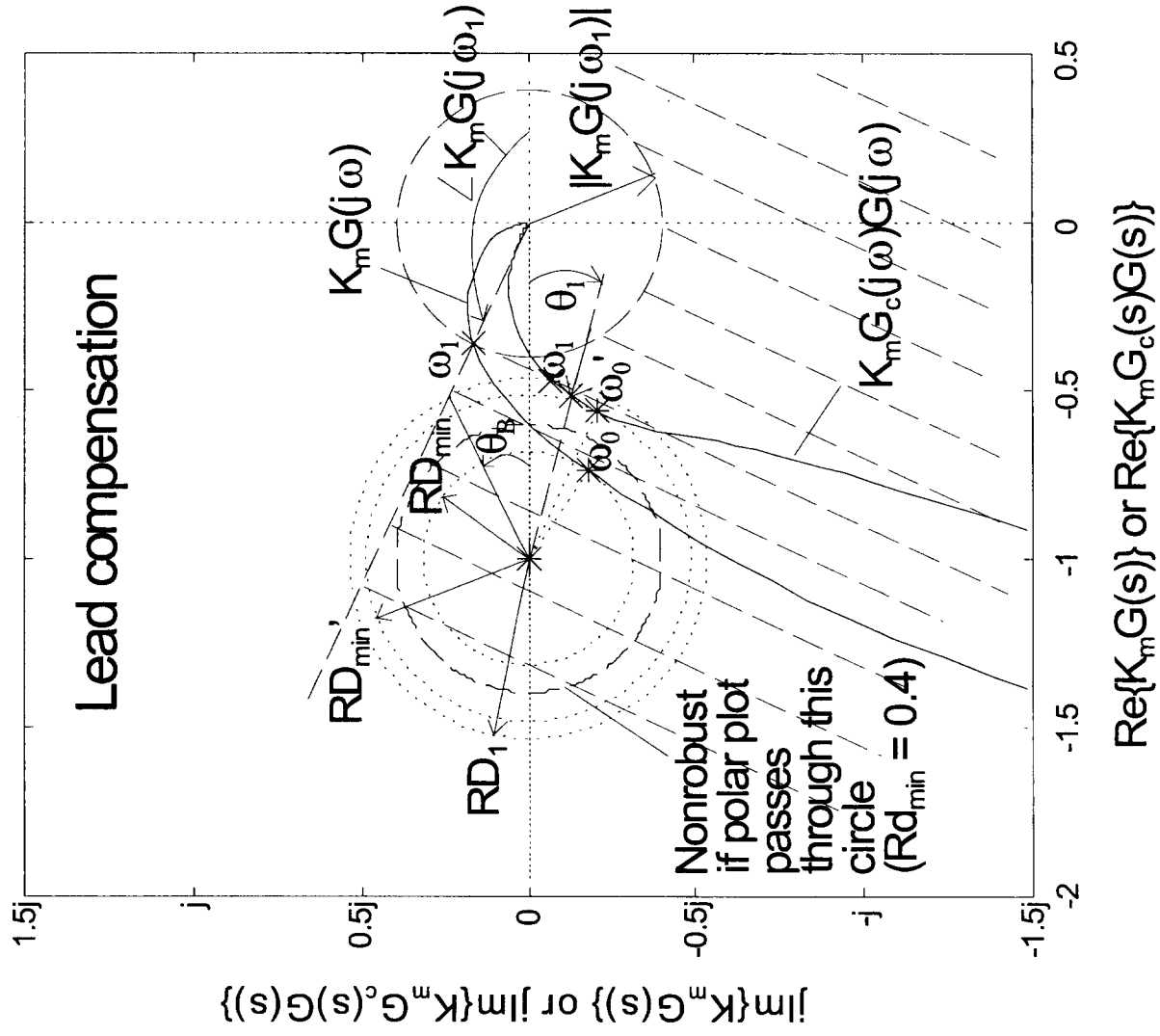


Figure (a)

